

Proton rich nuclei at and beyond the proton drip line in the Relativistic Mean Field theory

L.S. Geng^{1,2,*}, H. Toki^{1,†}, and J. Meng^{2,‡}

¹*Research Center for Nuclear Physics (RCNP),
Osaka University, Ibaraki, Osaka 567-0047, Japan*

²*School of Physics, Peking University, Beijing 100871, P.R. China*

Abstract

The Relativistic Mean Field theory is applied to the analysis of ground-state properties of deformed proton-rich odd-Z nuclei in the region $55 \leq Z \leq 73$. The model uses the TMA and NL3 effective interactions in the mean-field Lagrangian, and describes pairing correlations by the density-independent delta-function interaction. The model predicts the location of the proton drip line, the ground-state quadrupole deformation, one-proton separation energy at and beyond the proton drip line, the deformed single-particle orbital occupied by the odd valence proton and the corresponding spectroscopic factor. The results are in good agreement with the available experimental data except for some odd-odd nuclei in which the proton-neutron pairing may become important and are close to those of Relativistic Hartree-Bogoliubov model.

* E-mail address: lsgeng0@rcnp.osaka-u.ac.jp

† E-mail address: toki@rcnp.osaka-u.ac.jp

‡ E-mail address: mengj@pku.edu.cn

I. INTRODUCTION

The structure and decay modes of nuclei at and beyond the proton drip line represent one of the most active areas of experimental and theoretical studies of exotic nuclei with extreme isospin values. Recent reviews can be found in Ref [1, 2] and references therein. For each element there are minimum and maximum numbers of neutrons that can be supported by the nucleus, if the nucleus is to remain stable against nucleonic emission. These limits define the proton and neutron drip lines. Viewed from the perspective of the semi-empirical mass formula, the onset of neutron emission occurs when the gain in binding energy from a decrease in the symmetry energy overcomes the loss of volume binding energy, whereas for protons the decrease of electrostatic potential energy is a crucial determinant. Consequently the proton drip line lies much closer to the stability line than the neutron drip line does. For example, the lightest particle-stable neon is $^{17}_{10}\text{Ne}_7$ [1], while the isotope as heavy as $^{34}_{10}\text{Ne}_{24}$ [3] is known to exist.

The proton drip line is almost certainly fully mapped up to $Z = 21$ [1]. No proton-unbound nuclei have been directly observed in this region, which is not surprising since the Coulomb barrier is relatively low. It has been argued that ground-state proton decay can only be detected directly for nuclei with $Z > 50$, where the relatively high potential energy barrier causes nuclei to survive long enough to be detected by experiment [1]. Detailed studies of ground-state proton radioactivity have been reported for odd- Z nuclei mainly in the two mass regions, $51 \leq Z \leq 55$ and $69 \leq Z \leq 83$. The experimental features observed for most of these nuclei were explained by assuming them having spherical shapes [2]. The half-lives for proton decay were then evaluated using the semi-classical WKB method or standard reaction theory within the distorted wave approximation. However, proton decay rates in the transitional region beyond the $Z = 50$ shell closure (^{109}I and $^{112,113}\text{Cs}$) and in the region of light rare-earth nuclei (^{131}Eu and $^{140,141}\text{Ho}$) require calculations assuming significant prolate deformations. Recently, an exact formalism was developed in Ref. [4, 5], where the half-lives were evaluated with the assumption that the emitted proton moves in a deformed single particle Nilsson level. The formalism was applied [4, 5, 6, 7] to analyze all data presently known, on odd proton emitters with an even number of neutrons, and the known odd-odd proton emitters ^{112}Cs , ^{140}Ho and ^{150}Lu [8]. This formalism, however, does not predict proton separation energies, i.e., the model does not predict which nuclei

are likely to be proton emitters.

In the past decade, the Relativistic Mean Field (RMF) theory has been successfully applied to the study of nuclei throughout the periodic table. A general review of the RMF theory and its applications in nuclear physics can be found in Ref. [9, 10, 11]. For the study of drip-line nuclei, because the Fermi surface is close to the threshold, proper treatment of the continuum is essential for correct description of these nuclei. As suggested in Ref. [12, 13, 14, 15, 16, 17, 18], the use of a delta-function interaction, $V = -V_0\delta(\mathbf{r}_1 - \mathbf{r}_2)$, with both density independent and dependent couplings, could be an efficient and an economical way to obtain this aim. In our present work, the recently developed deformed RMF+BCS method [18] is applied to the analysis of deformed odd-Z proton-rich nuclei with $55 \leq Z \leq 73$. In the mean-field part, the most successful parameter sets TMA [19] and NL3 [20] are used.

The RMF theory was first applied to study deformed proton emitters by Lalazissis et al.. In their papers [21, 22, 23, 24], the proton drip-line nuclei with $31 \leq Z \leq 49$ and $51 \leq Z \leq 73$ have been studied within the framework of the Relativistic Hartree-Bogoliubov (RHB) model. In the mean-field part, the NL3 [20] parameter set is used. In the particle-particle channel, the pairing part of the Gogny force with the D1S set [25] has been adopted. The calculated one-proton separation energy and other relevant properties are in good agreement with the available experimental values. Such a success suggested that the RMF theory could be an appropriate method even for the description of nuclei with extreme isospin values. A natural question is whether or not such a success is dependent on a particular combination of parameter sets, i.e., NL3+D1S. Another question is whether or not the argument that a delta-function interaction is a good and efficient interaction to treat the pairing correlation still holds true in such extreme cases (proton drip line). We will compare our results with the available RHB results.

The article is organized as follows. In Section II, we give a brief introduction of the deformed RMF+BCS method. In Section III, we present our results for odd-Z proton-rich nuclei with $55 \leq Z \leq 73$ and compare our results with experiment and those of RHB method. Section IV is devoted to the summary of this paper.

II. THE DEFORMED RMF+BCS METHOD

Our RMF calculations have been carried out using the model Lagrangian density with nonlinear terms both for the σ and ω mesons as described in detail in Ref. [18]. The Lagrangian density is given by

$$\begin{aligned} \mathcal{L} = & \bar{\psi}(i\gamma^\mu\partial_\mu - M)\psi + \frac{1}{2}\partial_\mu\sigma\partial^\mu\sigma - \frac{1}{2}m_\sigma^2\sigma^2 - \frac{1}{3}g_2\sigma^3 - \frac{1}{4}g_3\sigma^4 - g_\sigma\bar{\psi}\sigma\psi \\ & - \frac{1}{4}\Omega_{\mu\nu}\Omega^{\mu\nu} + \frac{1}{2}m_\omega^2\omega_\mu\omega^\mu + \frac{1}{4}g_4(\omega_\mu\omega^\mu)^2 - g_\omega\bar{\psi}\gamma^\mu\psi\omega_\mu \\ & - \frac{1}{4}R_{\mu\nu}^aR^{a\mu\nu} + \frac{1}{2}m_\rho^2\rho_\mu^a\rho^{a\mu} - g_\rho\bar{\psi}\gamma_\mu\tau^a\psi\rho^{a\mu} \\ & - \frac{1}{4}F_{\mu\nu}F^{\mu\nu} - e\bar{\psi}\gamma_\mu\frac{1-\tau_3}{2}A^\mu\psi, \end{aligned} \quad (1)$$

where the field tensors of the vector mesons and of the electromagnetic field take the following forms:

$$\begin{cases} \Omega_{\mu\nu} = \partial_\mu\omega_\nu - \partial_\nu\omega_\mu \\ R_{\mu\nu}^a = \partial_\mu\rho_\nu^a - \partial_\nu\rho_\mu^a - 2g_\rho\epsilon^{abc}\rho_\mu^b\rho_\nu^c \\ F_{\mu\nu} = \partial_\mu A_\nu - \partial_\nu A_\mu \end{cases} \quad (2)$$

and other symbols have their usual meanings. Based on the single-particle spectrum calculated by the RMF method described above, we perform a state-dependent BCS calculation [26, 27]. The gap equation has a standard form for all the single particle states. i.e.,

$$\Delta_k = -\frac{1}{2}\sum_{k'>0}\frac{\bar{V}_{kk'}\Delta_{k'}}{\sqrt{(\varepsilon_{k'} - \lambda)^2 + \Delta_{k'}^2}}, \quad (3)$$

where $\varepsilon_{k'}$ is the single particle energy and λ is the Fermi energy, whereas the particle number condition is given by $2\sum_{k>0}v_k^2 = N$. In the present work we use for the pairing interaction a delta-function interaction, i.e.,

$$V = -V_0\delta(\mathbf{r}_1 - \mathbf{r}_2), \quad (4)$$

with the same strength V_0 for both protons and neutrons. The pairing matrix element for the delta-function interaction is given by

$$\bar{V}_{ij} = \langle i\bar{i}|V|j\bar{j}\rangle - \langle i\bar{i}|V|\bar{j}j\rangle = -V_0\int d^3r \left[\psi_i^\dagger\psi_i^\dagger\psi_j\psi_{\bar{j}} - \psi_i^\dagger\psi_i^\dagger\psi_{\bar{j}}\psi_j \right] \quad (5)$$

with nucleon wave function in the form

$$\psi_i(\mathbf{r}, t) = \begin{pmatrix} f_i(\mathbf{r}) \\ ig_i(\mathbf{r}) \end{pmatrix} = \frac{1}{\sqrt{2\pi}} \begin{pmatrix} f_i^+(z, r_\perp)e^{i(\Omega_i-1/2)\varphi} \\ f_i^-(z, r_\perp)e^{i(\Omega_i+1/2)\varphi} \\ ig_i^+(z, r_\perp)e^{i(\Omega_i-1/2)\varphi} \\ ig_i^-(z, r_\perp)e^{i(\Omega_i+1/2)\varphi} \end{pmatrix} \chi_{t_i}(t). \quad (6)$$

A detailed description of the deformed RMF+BCS method can be found in Ref. [18].

In the present study, nuclei with both even and odd number of protons (neutrons) need to be calculated. We adopt a simple blocking method, where the ground state of an odd system is described by the wave function,

$$\alpha_{k_1}^\dagger |BCS\rangle = \alpha_{k_1}^\dagger \prod_{k \neq k_1} (u_k + v_k \alpha_k^\dagger \alpha_k^\dagger) |vac\rangle, \quad (7)$$

Here, $|vac\rangle$ denotes the vacuum state. The unpaired particle sits in the level k_1 and blocks this level for pairing correlations. The Pauli principle prevents this level from participating in the scattering process of nucleons caused by the pairing correlations. As described in Ref. [27], in the calculation of the gap, one level is "blocked":

$$\Delta_k = -\frac{1}{2} \sum_{k' \neq k_1 > 0} \frac{\bar{V}_{kk'} \Delta_{k'}}{\sqrt{(\varepsilon_{k'} - \lambda)^2 + \Delta_{k'}^2}}. \quad (8)$$

The level k_1 has to be excluded from the sum, because it can not contribute to the pairing energy. The corresponding chemical potential, λ , is determined by

$$N = 1 + 2 \sum_{k \neq k_1 > 0} v_k^2. \quad (9)$$

The blocking procedure is performed in each step of the self-consistent iteration.

III. DEFORMED GROUND-STATE PROTON EMITTERS WITH $55 \leq Z \leq 73$

In the present work, we take the mass-dependent parameter set TMA [19] for the RMF Lagrangian. Results with parameter set NL3 [20] are also shown for comparison. For each nucleus, first the constrained quadrupole calculation [28, 29] is done to obtain all possible ground-state configurations, and then we perform the non-constrained calculation using the quadrupole deformation parameter of the deepest minimum of the energy curve of each nucleus as the deformation parameter for our Harmonic Oscillator basis. In the case of several similar minima from the constrained calculation, we repeat the above procedure to get the configuration with the lowest energy as our final result. We take the same pairing strength for both protons and neutrons in our work. The pairing strength is fixed by getting reasonable pairing gaps compared with experimental data. More specifically, for calculations with NL3 set we take $V_0 = 393.0$ MeV fm 3 when $Z \geq 71$, otherwise $V_0 = 420.0$ MeV fm 3 . For calculations with TMA set we take $V_0 = 393.0$ MeV fm 3 when $Z \geq 71$, otherwise $V_0 = 375.0$

MeV fm³. The calculations for the present analysis have been performed by an expansion in 14 oscillator shells for fermion fields and 20 shells for boson fields for those isotopes $Z \geq 70$, i.e., Ta and Lu isotopes. While for those isotopes $Z \leq 70$, 12 shells for fermion fields and 20 shells for boson fields are used. Following Ref. [30], we fix $\hbar\omega_0 = 41A^{-1/3}$ for fermions.

In the process of proton emission, the valence proton tunnels through the Coulomb and centrifugal barriers, and the decay probability depends strongly on the energy of the unbound proton and on its angular momentum. In rare-earth nuclei the decay of the ground state by direct proton emission competes with β^+ decay; for heavy nuclei fission or α decay can also be favored. In general, ground-state proton emission is not observed immediately after the proton drip line. For small values of the proton separation energies, the width is dominated by the β^+ decay. On the other hand, large separation energies result in extremely short proton emission half-lives, which are difficult to observe experimentally. For a typical rare-earth nucleus, the separation energy window, in which ground-state proton decay can be directly observed, is about 0.8 – 1.7 MeV [2].

The Nilsson quantum numbers of the odd-proton level are determined by the dominant component in the expansion of this wave function in terms of the anisotropic oscillator basis [18]. On the theoretical side, the spectroscopic factor of the deformed odd-proton orbital k is defined as the probability that this state is found empty in the daughter nucleus with even number of protons. If one neglects the difference between the ground-state configuration for the even- and the odd-proton system, the spectroscopic factor of level k is calculated as

$$S_k = | < \Phi | \alpha_k | \Phi_k > |^2 = u_k^2, \quad (10)$$

where u_k is determined in the single particle basis of the daughter nucleus with even proton numbers. In the BCS case, u_k^2 is related to the occupation probability v_k^2 through the well-known relation

$$u_k^2 + v_k^2 = 1. \quad (11)$$

In what follows, we discuss the details of our numerical results.

A. Lutetium(Z=71) and Tantalum(Z=73)

The one-proton separation energies for Lu and Ta isotopes are displayed in Fig. 1 as a function of mass number A . The predicted drip-line nucleus for Ta is ¹⁶⁰Ta by NL3 and

^{161}Ta by TMA. While for Lu, both TMA and NL3 predict the drip-line nucleus to be ^{156}Lu . We also compare the calculated separation energies with available experimental transition energies for ground-state proton emission in ^{150}Lu , ^{151}Lu [32], ^{155}Ta [33], ^{156}Ta [34] and ^{157}Ta [35]. The corresponding RHB results are taken from Ref. [21]. In Table. I, we list the ground-state properties of Lu and Ta isotopes. The separation energy window, 0.8-1.7 MeV, extends to include those nuclei for which a direct observation of ground-state proton emission is in principle possible on the basis of our calculated separation energies. Good agreement between our calculation and both the experimental values and the RHB results can be clearly seen. However, for the odd-odd nuclei ^{150}Lu and ^{156}Ta , our calculations predict smaller S_p compared with experiment. This can be explained by a possible existence of residual proton-neutron pairing interaction. In both nuclei, an extra positive energy of about 0.3 MeV is needed to raise the calculated S_p to the experimental value. We find if we reduce the pairing strength for odd-odd nuclei by about $5 \sim 10$ percent compared with odd-even or even-even nuclei, we can reproduce the experimental transition energy quite well. We can see later the same conclusion also holds as well for other odd-odd nuclei. Although it has long been believed that proton-neutron pairing is important for proper description of nuclei [36, 37], it was believed it only affects those proton-rich nuclei with $N \approx Z$. However, recently Šimkovic et al. [38] show that even for nuclei with $N - Z = 12$, the proton-neutron pairing can not be ignored.

As for the deformation, both RMF+BCS method and RHB model predict oblate shapes for Lu proton emitters, and similar values for the ground-state quadrupole deformations. Recent calculations by Ferreira et al. [6] show that proton decay from ^{151}Lu can be described very well as decay from a $K = 5/2^-$ ground state with an oblate deformation, $-0.18 < \beta_2 < -0.14$. In another work [8], the author finds proton decay from ^{150}Lu is very well described as decay from a $K = 5/2^-$ ground state with an oblate deformation, $-0.17 < \beta_2 < -0.16$. These calculations are in good agreement with our predictions. In the calculations of RHB model, Ta isotopes are assumed to be spherical, while they are slightly deformed in our calculations. At first sight, RMF+BCS/TMA and RHB model predict quite different p-orbital for ^{157}Ta , ^{156}Ta , and ^{155}Ta , but in fact these states are quite close to each other in our calculations. The theoretical predictions are compared with the corresponding experimental assignments for the ground-state configuration and spectroscopic factor. The experimental values for ^{155}Ta [33], ^{156}Ta [2] and ^{157}Ta [2] are respectively $11/2^-$, 0.58(20); $3/2^+$, 0.67(16)

and $1/2^+$, 0.74(34). We notice that the experimental assignments are somehow different both from our predictions, where $^{155-157}\text{Ta}$ are slightly deformed, and from RHB calculations, where spherical shapes are assumed. The reasons could be two fold: first, these states are close to each other in our calculations so that a clear distinction is difficult; second, deformation could change the state occupied by the odd-proton somehow. Since the nuclei $^{155-157}\text{Ta}$ are not strongly deformed, a different combination of deformation and occupied state can give the same experimental observed values, i.e., the experimental transition energy and decay half-lives.

B. Holmium(Z=67) and Thulium(Z=69)

In Fig. 2, we show one-proton separation energies for Ho and Tm isotopes as a function of mass number, A. Available experimental values for ^{147}Tm [32], ^{146}Tm [39], ^{145}Tm [40], ^{140}Ho [41] and ^{141}Ho [42], together with results of RHB calculations [22] are also shown for comparison. The predicted drip-line nucleus for Tm isotope is ^{152}Tm , while for Ho isotope, NL3 predicts ^{146}Ho and TMA predicts ^{144}Ho . From Fig. 2, we see both RMF+BCS/TMA and RHB method predict a smaller transition energy value for ^{141}Ho , while RMF+BCS/NL3 predicts a better S_p compared with the experimental value. Nevertheless, all theoretical calculations failed to produce the increase of one-proton separation energy from ^{141}Ho to ^{140}Ho . This can be corrected by reducing the pairing strength by a few percent as we have mentioned above. However, this is not our aim here. It is clear, even after changing the pairing strength, we can not reproduce the trend from ^{141}Ho to ^{140}Ho , which has been attributed to the residual proton-neutron interaction in our above analysis. In Table. II, we list properties of proton emitters for Ho and Tm isotopes. We see that our RMF+BCS/TMA method predict an oblate shape for ^{145}Tm , while RHB method predicted a prolate shape. In fact, in our constrained calculation, both prolate and oblate shapes are possible for ^{145}Tm and ^{144}Er . This is illustrated in Fig. 3, where we plot the binding energy per particle for ^{145}Tm and ^{144}Er as a function of the quadrupole deformation parameter, β_{2m} [18]. The binding energies result from the RMF+BCS/TMA calculations performed by imposing a quadratic constraint on the quadrupole moment. We find two similar minima around $\beta_2 \approx -0.22$ and $\beta_2 \approx 0.25$ for both ^{145}Tm and ^{144}Er . More specifically, two minima for ^{145}Tm are: $\beta_{2m} = 0.287$, $E/A = -7.906$; $\beta_{2m} = -0.211$, $E/A = -7.903$; and for ^{144}Er :

$\beta_{2m} = 0.303$, $E/A = -7.767$; $\beta_{2m} = -0.196$, $E/A = -7.768$. The reason why we choose the oblate shape instead of the prolate shape for ^{145}Tm is two fold. First, we would like to choose the same shape for both ^{145}Tm and ^{144}Er . Second, the oblate shape for ^{145}Tm is more consistent with its neighbors (see also Fig. 7). We note that unlike Lu and Ta isotopes both RMF+BCS/TMA and RHB predict the same last occupied odd-proton state for Ho and Tm isotopes (see also Table. II).

C. Europium(Z=63) and Terbium(Z=65)

In Fig. 4, we plot one-proton separation energies for Tb and Eu isotopes. The results of RHB model [21, 22] and the only available experimental value for ^{131}Eu [42] are also shown. Predicted drip-line nucleus for Tm isotope is ^{140}Tb for NL3 and ^{139}Tb for TMA. While for Eu isotope, the drip-line nucleus is ^{133}Eu predicted for TMA and ^{134}Eu predicted for NL3. In this region, only one proton emitter, ^{131}Eu , has been reported. However, based on our calculations, there are three other possible proton emitters, ^{130}Eu , ^{135}Tb and ^{136}Tb . We list their properties in Table. III. We notice that the experimental transition energy for ^{131}Eu is 0.950(8) MeV, while our RMF+BCS/TMA calculations predict 0.498 MeV. This can be corrected by adjusting the pairing strength slightly. Considering this correction, we see both RHB and RMF+BCS predict similar proton emitters for Tb and Eu isotopes. As we can see up to now, the description of proton emitters is quite sensitive to the pairing strength. We hope that further experimental measurements of proton emitters in the whole region can help us to understand more about the pairing interaction in the exotic nuclei.

D. Praseodymium(Z=59) and Promethium(Z=61)

In Fig. 5, one-proton separation energies for Pm and Pr isotopes are plotted against mass number A, together with the results of RHB model [21, 22]. The predicted drip-line nuclei are ^{128}Pm and ^{125}Pr for both TMA and NL3. No experimental proton emitters have been reported for these two isotopes. Based on our calculations, possible proton emitters in this region are $^{119,120}\text{Pr}$ and $^{124,125}\text{Pm}$. The properties of these nuclei are listed in Table. IV.

E. Cesium(Z=55) and Lanthanum(Z=57)

In Fig. 6, we plot one-proton separation energies for Cs and La isotopes. The results of RHB model [21, 22] are shown for comparison. Predicted drip-line nuclei are ^{115}Cs and ^{118}La for TMA, ^{115}Cs and ^{119}La for NL3. In Figure. 6, we see that the latest reported proton emitter ^{117}La [44, 45] is reproduced quite well by RMF+BCS/NL3. Both RHB and RMF+BCS fail to reproduce the experimental data for ^{112}Cs . As we have mentioned above, ^{112}Cs has an odd number of protons and an odd number of neutrons. Since $N - Z$ is only 2, one expects a relatively strong interaction between the odd proton and the odd neutron. Compared with the odd-even system, the additional interaction will increase the binding energy. Since the two mean-field models, RHB and RMF+BCS, do not include any residual proton-neutron interaction, they can not reproduce the inversion of separation energies. As also suggested by Ref. [22] that such an additional interaction could be represented by a surface delta-function interaction. According to our calculations, remaining possible proton emitters in La isotopes are ^{115}La and ^{116}La as listed in Table. V.

F. Quadrupole deformation

The calculated mass quadrupole deformation parameter, β_{2m} , for the odd-Z and even-Z nuclei with $54 \leq Z \leq 73$ at and beyond the proton drip line are shown in Fig. 7 as a function of neutron number, N . While prolate deformations $0.15 \leq \beta_{2m} \leq 0.25$ are calculated for Cs isotopes, the proton-rich isotopes of La, Pr, Pm, Eu and Tb are strongly deformed ($0.35 \leq \beta_2 \leq 0.45$). By increasing the number of neutrons, Ho isotopes display a transition from prolate to oblate shapes, while most of Tm nuclei have oblate shapes. Lu and Ta isotopes show a transition from oblate to prolate shapes. The absolute value of β_{2m} decreases as neutron number approach the traditional magic number $N = 82$.

For stable even-even nuclei, the information of deformation parameter can be derived from the measurements of $B(E2) \uparrow$ values. The $B(E2) \uparrow$ values are basic experimental quantities that do not depend on nuclear models. Assuming a uniform charge distribution out to the distance $R(\theta, \phi)$ and zero charge beyond, β_{2p} is related to $B(E2) \uparrow$ by

$$\beta_{2p} = (4\pi/3ZR_0^2)[B(E2) \uparrow /e^2]^{1/2}, \quad (12)$$

where R_0 has been taken to be $1.2A^{1/3}$ fm and $B(E2) \uparrow$ is in units of e^2b^2 . Unfortunately,

we do not have much knowledge about the $B(E2) \uparrow$ values for proton drip-line nuclei. The two available experimental values [46] in the region are $\beta_{2p} = 0.221(7)$ for ^{114}Xe and $\beta_{2p} = 0.385(48)$ for ^{124}Ce , which are in good agreement with our calculations: $\beta_{2p} = 0.199$ for ^{114}Xe and $\beta_{2p} = 0.344$ for ^{124}Ce (see also Fig. 7).

Another source of our knowledge for the deformation of proton drip-line nuclei can be obtained from the analysis of properties of proton emitters as shown in Ref. [4, 5, 6, 7, 8]. In those calculations, a basic assumption is that the parent nucleus and daughter nucleus have the same deformation. Our calculations show for Ho, Tm, Lu and Ta isotopes, the parent and daughter nucleus have almost the same deformation. However, for other six isotopes, an absolute deviation of $0.02 \sim 0.09$ is found to exist. To what extent such a deviation can influence the conclusions of those calculations [4, 5, 6, 7, 8] need to be studied in more detail.

IV. CONCLUSION

The deformed RMF+BCS method with density-independent delta-function interaction in the pairing channel has been adopted to study the ground-state properties of proton emitters with $55 \leq Z \leq 73$. The principle advantage of working in the relativistic framework is its ability to describe all the nuclear mean fields in a unified and fully self-consistent way. In particular, the spin-orbit term of the effective single-nucleon potential is automatically included in the Relativistic Mean Field model. In contrast to non-relativistic models, the strength and isospin dependence of the spin-orbit interaction do not require the introduction of additional free parameters. With a delta-function interaction in the pairing channel, which can include the continuum effect properly, this model provides a unified and self-consistent description of mean-field and pairing interactions. This model is especially important for applications in exotic nuclei far from the β -stability line.

In the present work, this model has been used to study the location of the proton drip line, the ground-state quadrupole deformation, one-proton separation energy at and beyond the proton drip line, the deformed single-particle orbital occupied by the odd valence proton and the corresponding spectroscopic factor. The RMF+BCS model reproduce the available data very well except for odd-odd nuclei in which the proton-neutron pairing may become important and are in good agreement with those of Relativistic Hartree-Bogoloubov model.

Predicted drip-line nuclei by RMF+BCS/TMA calculations are respectively: ^{161}Ta , ^{156}Lu , ^{152}Tm , ^{144}Ho , ^{139}Tb , ^{133}Eu , ^{129}Pm , ^{125}Pr , ^{118}La and ^{115}Cs . Based on our calculations, possible proton emitters that could be detected by future experiments are: ^{149}Lu , ^{152}Lu , ^{153}Lu and ^{154}Lu for Lu isotopes; ^{158}Ta for Ta isotopes; ^{130}Eu for Eu isotopes; ^{135}Tb and ^{136}Tb for Tb isotopes; ^{119}Pr and ^{120}Pr for Pr isotopes; ^{124}Pm and ^{125}Pm for Pm isotopes; ^{111}Cs for Cs isotopes; ^{115}La and ^{116}La for La isotopes.

V. ACKNOWLEDGMENTS

L.S. Geng is grateful to the Monkasho fellowship for supporting his stay at Research Center for Nuclear Physics where this work is done .

- [1] P.J. Woods and C.N. Davids, *Annu. Rev. Nucl. Part. Sci.* 47 (1997) 541.
- [2] S. Aberg, P.B. Semmes, and W. Nazarewicz, *Phys. Rev. C* 56 (1997) 1762.
- [3] M. Notani et al., *Phys. Lett. B* 542 (2002) 49.
- [4] E. Maglione, L.S. Ferreira, and R.J. Liotta, *Phys. Rev. Lett.* 81 (1998) 538.
- [5] E. Maglione, L.S. Ferreira, and R.J. Liotta, *Phys. Rev. C* 59 (1999) R589.
- [6] L.S. Ferreira and E. Maglione, *Phys. Rev. C* 61 (2000) R021304.
- [7] E. Maglione and L.S. Ferreira, *Phys. Rev. C* 61 (2000) 047307.
- [8] L.S. Ferreira and E. Maglione, *Phys. Rev. Lett.* 86 (2001) 1721.
- [9] B.D. Serot and J.D. Walecka, *Adv. Nucl. Phys.* 16 (1986) 1.
- [10] P.G. Reinhard, *Rep. Prog. Phys.* 52 (1989) 439.
- [11] P. Ring, *Prog. Part. Nucl. Phys.* 37 (1996) 193.
- [12] J. Meng and P. Ring, *Phys. Rev. Lett.* 77 (1996) 3963.
- [13] J. Meng and P. Ring, *Phys. Rev. Lett.* 80 (1998) 460.
- [14] J. Meng, *Nucl. Phys. A* 635 (1998) 3.
- [15] J. Meng, H. Toki, J. Y. Zeng, S.Q. Zhang and S.G. Zhou, *Phys. Rev. C* 65 (2002) R041302.
- [16] H. L. Yadav, S. Sugimoto and H. Toki, *Mod. Phys. Lett. A* 17 (2002) 2523.
- [17] N. Sandulescu, Nguyen Van Giai, and R. J. Liotta, *Phys. Rev. C* 61 (2000) R061301.
- [18] L.S. Geng, H. Toki, S. Sugimoto and J. Meng, *arXiv:nucl-th/0306038*.

- [19] Y. Sugahara and H. Toki, A 579 (1994) 557, Y. Sugahara, Doctor thesis in Tokyo Metropolitan University (1995).
- [20] G. A. Lalazissis, J. König, and P. Ring, Phys. Rev C 55 (1997) 540.
- [21] G.A. Lalazissis, D. Vretenar and P. Ring, Phys. Rev. C 60 (1999) R051302.
- [22] G.A. Lalazissis, D. Vretenar, P. Ring, Nucl. Phys. A 650 (1999) 133-156.
- [23] D. Vretenar, G.A. Lalazissis and P. Ring, Phys. Rev. Lett. 82 (1999) 4595.
- [24] G.A. Lalazissis, D. Vretenar, P. Ring, Nucl. Phys. A 679 (2001) 481-493.
- [25] J.F. Berger, M. Girod, D. Gogny, Nucl. Phys. A 428 (1984) 23c-36c.
- [26] A. M. Lane, *Nuclear Theory* (Benjamin, 1964).
- [27] P. Ring and P. Schuck, *The Nuclear Many-Body Problem* (Springer, 1980).
- [28] F. Floard et al., Nucl. Phys. A 203 (1973) 433.
- [29] D. Hirata, K. Sumiyoshi, I. Tanihata, Y. Sugahara, T. Tachibana and H. Toki, Nucl. Phys. A 616 (1997) 438c.
- [30] Y.K. Gambhir, P. Ring and A. Thimet, Ann. Phys. (N.Y.) 194 (1990) 132.
- [31] S. Hofmann, in *Nuclear Decay Modes*, edited by D.N. Poenaru and W. Greiner (IOP, Bristol, 1996).
- [32] P.J. Sellin et al, Phys. Rev. C 47 (1993) 1933.
- [33] J. Uusitalo et al., Phys. Rev. C 59 (1999) R2975.
- [34] R.D. Page et al., Phys. Rev. Lett. 68 (1992) 1287.
- [35] R.J. Irvine et al., Phys. Rev. C 55 (1997) R1621.
- [36] H.T. Chen, and A. Goswami, Phys. Lett. B 24 (1967) 257.
- [37] A.L. Goodman, Nucl. Phys. A 186 (1972) 475-492.
- [38] F. Šimkovic, Ch.C. Moustakidis, L. Pacearescu, and Amand Faessler, *arXiv:nucl-th/0308046*.
- [39] K. Livingston et al., Phys. Lett. B 312 (1993) 46.
- [40] J.C. Batchelder et al., Phys. Rev. C 57 (1998) R1042.
- [41] K. Rykaczewski et al., Phys. Rev. C 60 (1999) R011301.
- [42] C.N. Davids et al., Phys. Rev. Lett. 80 (1998) 1849.
- [43] R.D. Page et al., Phys. Rev. Lett. 72 (1994) 1798.
- [44] H. Mahmud et al., Phys. Rev. C 64 (2001) R031303.
- [45] F. Soramel et al, Phys. Rev. C 63 (2001) R031304.
- [46] S. Raman, C.W. Nestor, JR., and P. Tikkainen, At. Data Nucl. Data Tables 78 (2001) 1.

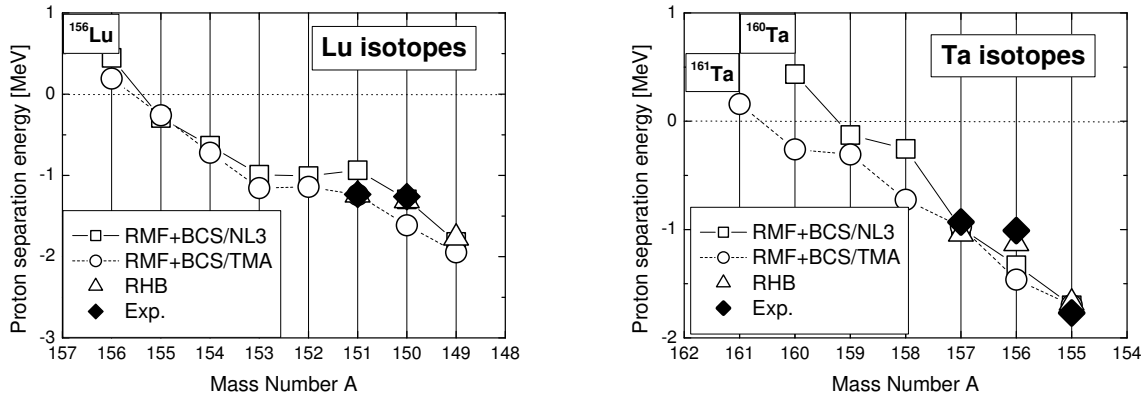


FIG. 1: One-proton separation energies for Lu ($Z=71$) and Ta ($Z=73$) isotopes at and beyond the proton drip line. The experimental value for the proton separation energy correspond to the negative value of the ground-state transition energy, E_p .

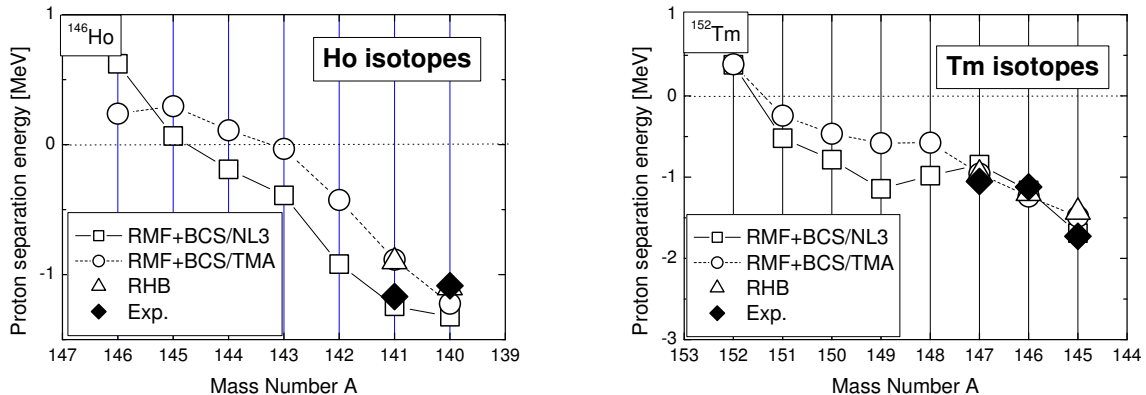


FIG. 2: The same as Fig. 1, but for Ho ($Z=67$) and Tm ($Z=69$) isotopes.

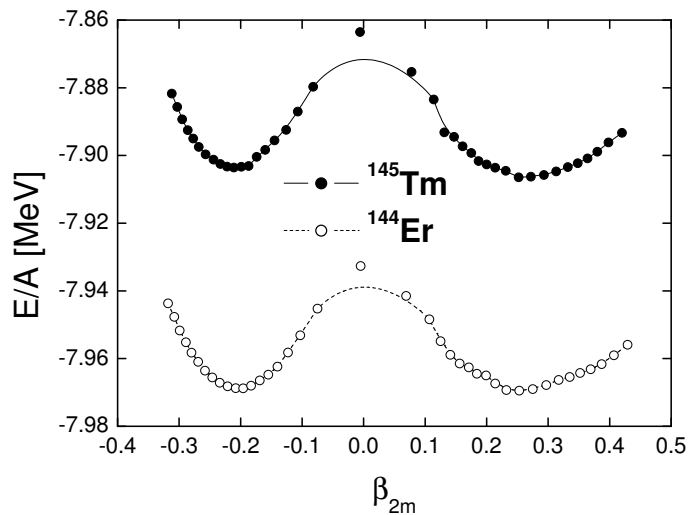


FIG. 3: Binding energy per particle, E/A , for ^{145}Tm and ^{144}Er , are plotted against mass quadrupole deformation parameter, β_{2m} .

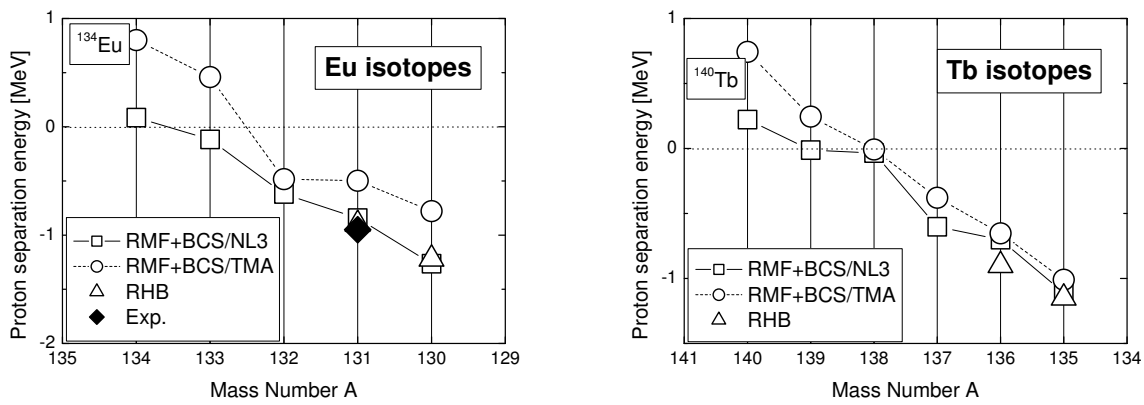


FIG. 4: The same as Fig. 1, but for Eu ($Z=63$) and Tb ($Z=65$) isotopes.

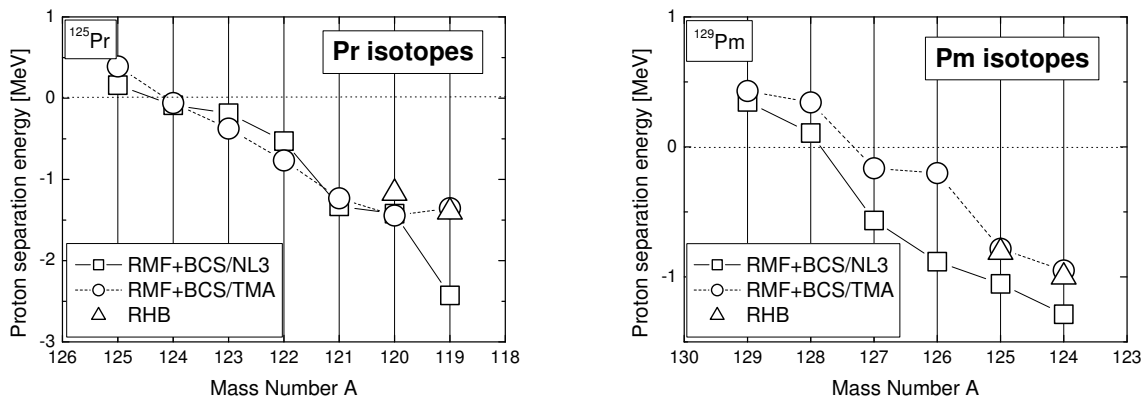


FIG. 5: The same as Fig. 1, but for Pr ($Z=59$) and Pm ($Z=61$) isotopes.

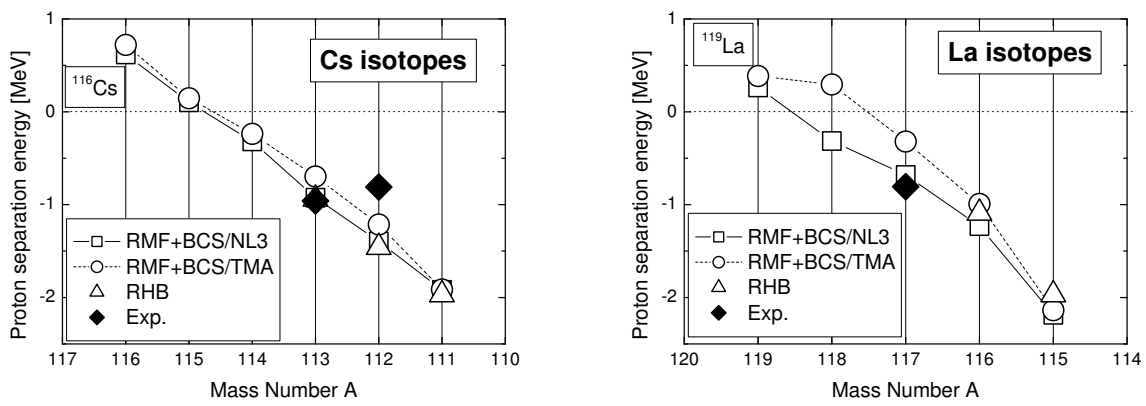


FIG. 6: The same as Fig. 1, but for Cs ($Z=55$) and La ($Z=57$) isotopes.

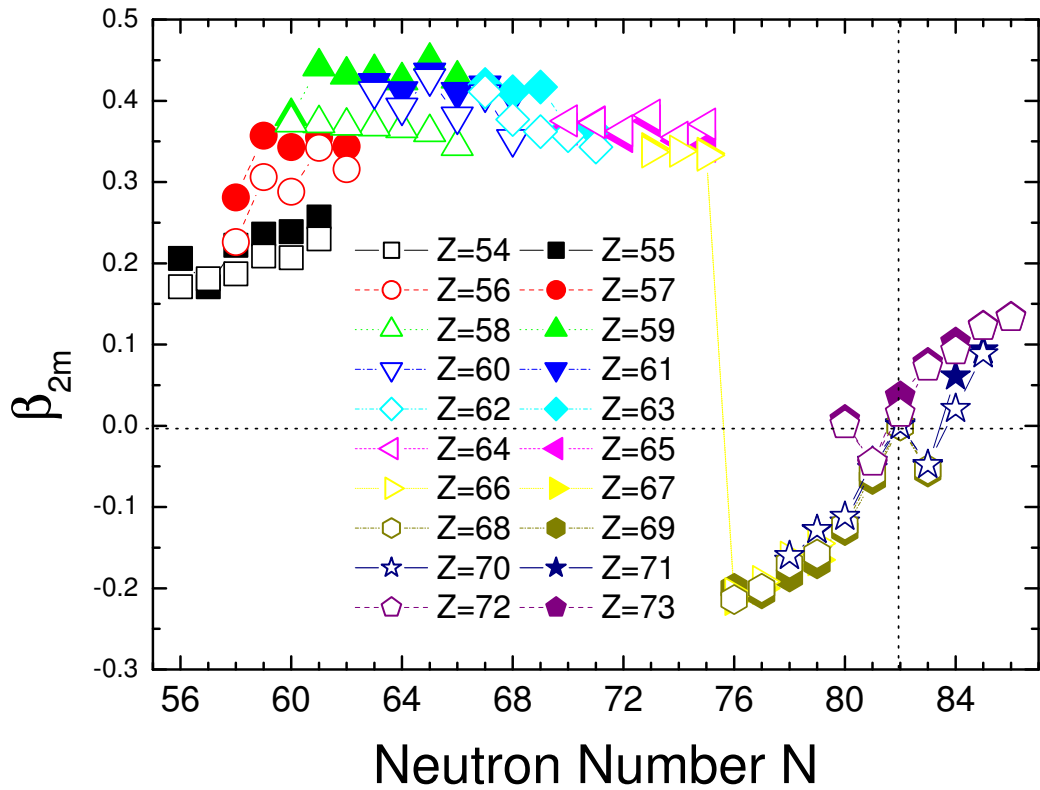


FIG. 7: Ground-state quadrupole deformations for proton drip-line nuclei with $54 \leq Z \leq 73$ as a function of neutron number, N , at and beyond the proton drip line.

TABLE I: Lu (Z=71) and Ta (Z=73) ground-state proton emitters. The results of RMF+BCS/TMA calculations (third to sixth column) for one-proton separation energy S_p , mass quadrupole deformation β_2 , and the deformed single-particle orbit occupied by the odd valence proton, are compared with predictions of RHB model [21] (seventh to tenth column) and with experimental value $S_p = -E_p$, where E_p is the experimental transition energy. The RMF+BCS/TMA and RHB spectroscopic factors are displayed in the sixth and tenth columns respectively. All energies are given in unit of MeV.

		RMF+BCS/TMA				RHB				Exp.
N		S_p	β_2	p orbital	u^2	S_p	β_2	p orbital	u^2	S_p
^{149}Lu	78	-1.946	-0.166	$5/2^-$ [512]	0.574	-1.77	-0.158	$7/2^-$ [523]	0.60	
^{150}Lu	79	-1.613	-0.129	$5/2^-$ [523]	0.549	-1.31	-0.153	$7/2^-$ [523]	0.61	-1.261(4) [32]
^{151}Lu	80	-1.239	-0.119	$5/2^-$ [532]	0.541	-1.24	-0.151	$7/2^-$ [523]	0.58	-1.233(3) [32]
^{152}Lu	81	-1.141	-0.053	$5/2^-$ [532]	0.496					
^{153}Lu	82	-1.156	0.002	$7/2^-$ [523]	0.463					
^{154}Lu	83	-0.720	-0.050	$5/2^-$ [532]	0.513					
^{155}Ta	82	-1.698	0.007	$9/2^-$ [514]	0.374	-1.677	0.000	$11/2^-$	0.60	-1.765(10) [33]
^{156}Ta	83	-1.462	-0.048	$3/2^-$ [521]	0.437	-1.129	0.000	$3/2^+$	0.51	-1.007(5) [34]
^{157}Ta	84	-0.974	0.036	$9/2^-$ [514]	0.381	-1.040	0.000	$11/2^-$	0.42	-0.927(7) [35]
^{158}Ta	85	-0.725	0.077	$9/2^-$ [514]	0.470					

TABLE II: The same as Table. I, but for Ho (Z=67) and Tm (Z=69) isotopes.

		RMF+BCS/TMA				RHB				Exp.
N		S_p	β_2	p orbital	u^2	S_p	β_2	p orbital	u^2	S_p
^{140}Ho	73	-1.223	0.341	$7/2^-$ [523]	0.592	-1.10	0.31	$7/2^-$ [523]	0.61	-1.086(10) [41]
^{141}Ho	74	-0.885	0.339	$7/2^-$ [523]	0.594	-0.90	0.32	$7/2^-$ [523]	0.64	-1.169(8) [42]
^{145}Tm	76	-1.458	-0.220	$7/2^-$ [523]	0.458	-1.43	0.23	$7/2^-$ [523]	0.47	-1.728(10) [40]
^{146}Tm	77	-1.238	-0.207	$7/2^-$ [523]	0.460	-1.20	-0.21	$7/2^-$ [523]	0.50	-1.120(10) [39]
^{147}Tm	78	-0.958	-0.186	$7/2^-$ [523]	0.467	-0.96	-0.19	$7/2^-$ [523]	0.55	-1.054(19) [32]

TABLE III: The same as Table. I, but for Eu (Z=63) and Tb (Z=65) isotopes.

		RMF+BCS/TMA				RHB				Exp.
N		S_p	β_2	p orbital	u^2	S_p	β_2	p orbital	u^2	S_p
130 Eu	67	-0.778	0.420	$5/2^+[413]$	0.464	-1.22	0.34	$5/2^-[532]$	0.44	
131 Eu	78	-0.498	0.411	$5/2^+[413]$	0.323	-0.90	0.35	$5/2^+[413]$	0.44	-0.950(8) [42]
135 Tb	70	-1.01	0.365	$3/2^+[411]$	0.879	-1.15	0.34	$3/2^+[411]$	0.62	
136 Tb	71	-0.653	0.374	$3/2^+[411]$	0.862	-0.90	-0.32	$3/2^+[411]$	0.65	

TABLE IV: The same as Table. I, but for Pr (Z=59) and Pm (Z=61) isotopes.

		RMF+BCS/TMA				RHB				Exp.
N		S_p	β_2	p orbital	u^2	S_p	β_2	p orbital	u^2	S_p
119 Pr	60	-1.354	0.381	$3/2^-[541]$	0.436	-1.40	0.32	$3/2^-[541]$	0.39	
120 Pr	61	-1.445	0.442	$9/2^+[404]$	0.107	-1.17	0.33	$3/2^-[541]$	0.33	
124 Pm	63	-0.95	0.422	$5/2^-[532]$	0.789	-1.00	0.35	$5/2^-[532]$	0.72	
125 Pm	64	-0.783	0.412	$5/2^-[532]$	0.800	-0.81	0.35	$5/2^-[532]$	0.74	

TABLE V: The same as Table. I, but for Cs (Z=55) and La (Z=57) isotopes.

		RMF+BCS/TMA				RHB				Exp.
N		S_p	β_2	p orbital	u^2	S_p	β_2	p orbital	u^2	S_p
111 Cs	56	-1.913	0.206	$1/2^+[420]$	0.949	-1.97	0.20	$1/2^+[420]$	0.74	
112 Cs	57	-1.213	0.171	$5/2^+[413]$	0.906	-1.46	0.20	$1/2^+[420]$	0.74	-0.807(7) [43]
113 Cs	58	-0.697	0.222	$1/2^+[420]$	0.94	-0.94	0.21	$1/2^+[420]$	0.73	-0.9593(37) [40]
115 La	58	-2.136	0.281	$1/2^-[550]$	0.994	-1.97	0.26	$3/2^-[541]$	0.20	
116 La	59	-0.992	0.357	$3/2^-[541]$	0.8	-1.09	0.30	$3/2^-[541]$	0.73	
117 La	59	-0.32	0.343	$1/2^+[420]$	0.58					-0.806(5) [44]